Plasmonic Photodetectors

Alexander Dorodnyy, Yannick Salamin, Ping Ma, Jelena Vukajlovic Plestina, Nolan Lassaline, Dmitry Mikulik, Pablo Romero-Gomez, Anna Fontcuberta i Morral, and Juerg Leuthold, *Fellow, IEEE*

(Invited Paper)

***Abstract*—Plasmonic photodetectors are attracting the attention of the photonics community. Plasmonics is attractive because metallic structures have the ability to confine light by coupling an electromagnetic wave to charged carrier oscillations at the surface of the metal. The wavelength of such oscillations can be much smaller than the corresponding light wavelength in vacuum. This enables the light-matter interaction on a deep subwavelength scale, which in turn allows for more compact and potentially higher speed devices. In this review, we discuss different types of photodetectors and ways in which plasmonics can be applied to them. We elucidate several plasmonic photodetector concepts/schemes and discuss the main physical principles behind their operation. Finally, we reflect on the characteristics of an "ideal" photodetector and propose a device that might be the perfect plasmonic detector.**

***Index Terms*—Photodetectors, plasmons, waveguides, Schottky diodes, nanotechnology, nanowires, uni-traveling-carrier, silicon-compatible photonics.**

I. Introduction

PLASMONICS has received a lot of attention in the last decades. By utilizing the ability of metals to constrain light at a deep-subwavelength scale, plasmonics has already allowed to considerably shrink the device size of photonic components [1]–[8]. This size reduction brings the technology one step closer to a fusion of optical and electronic components at the same size scale [9]. This opens a path to a new generation of ultra-dense interconnects [10] with monolithically integrated optoelectronic interfaces. In addition, plasmonics might be a path to boost the operation speed [11]–[13]. And indeed, ultra-fast photodetectors are of high demand in the telecommunications and sensing market [14]; in the former to decode optical high-speed signals, and in the latter to be used when high-speed detection is required [15].

In recent years, many different plasmonic designs have been proposed in a wide range of photonic applications from the THz region to the ultraviolet [2], [8], [16]–[19]. Plasmonic components have already found applications as band-pass filters in various sensors and other color-sensitive elements [20], [21], to make lasers [22], [23], to concentrate light in order to increase absorption in 2D-materials [24]–[26], to enhance photoemission in hot-carrier detectors [16], [27], [28] and in various other applications where a high light concentration (strong light confinement) is required [29]–[33].

Here, we review and assess different plasmonic photodetector concepts. We have divided them according to the absorption material, the detection type and the plasmonic enhancement concept. We then discuss advantages of each concept and subsequently illustrate the principle with important examples. Finally, we propose a plasmonically enhanced uni-traveling-carrier (UTC)-nanowire photodetector to complement the current plasmonic schemes by an ultra-fast, low dark current detector with a large dynamic range that is compatible with the silicon platform.

II. Photodetector – A Classification

Plasmonic photodetectors naturally include metallic elements. The role of such elements can be of two kinds: (1) Metals can constitute the absorber in hot-carrier devices; (2) Metals can provide enhancement of electromagnetic field inside an absorber. Fig. 1 shows a simplified classification graph of plasmonic photodetectors. We first differentiate between detectors that rely on semiconductors or metals (hot-carrier photodetector type) as an absorber. We then classify photodetectors according to one of four basic operation schemes: The photoconductor detector, the p-i-n detector, the tunnel-junction, and the Schottky-detector. The Schottky and tunnel-junction operation schemes are also found in plasmonic hot-carrier detectors. Last, each of the detector types can be plasmonically enhanced by three basic forms: By a localized plasmon polarition in a metallic nanoparticle, by a surface plasmonic polariton (SPP) in a waveguide, or by a grating type plasmon. Note that both semiconductor and hot-carrier photodetectors may adopt plasmonic field enhancement schemes to maximize the efficiency [34], [35].

Manuscript received February 9, 2018; revised April 9, 2018; accepted May 15, 2018. Date of publication May 24, 2018; date of current version June 27, 2018. This work was supported in part by the ERC PLASILOR under Grant 670478, in part by the European Commission Horizon under Grant 688166, Grant 702629, and Grant 780997, in part by the SNF (PADOMO, precoR), in part by the H2020 (Indeed project), and in part by the ERANET-Russia SNF Program under Grant IZLRZ2_163861. *(Corresponding author: Alexander Dorodnyy.)*

A. Dorodnyy, Y. Salamin, P. Ma, and J. Leuthold are with the Institute of Electromagnetic Fields, ETH Zurich, Zürich 8092, Switzerland (e-mail: dorodnya@ethz.ch; salaminy@ethz.ch; ping.ma@ief.ee.ethz.ch; leuthold@ethz.ch).

J. Vukajlovic Plestina, D. Mikulik, P. Romero-Gomez, and A. Fontcuberta i Morral are with the Laboratory of Semiconductor Materials, EPFL Lausanne, Lausanne 1015, Switzerland (e-mail: jelena.vukajlovicplestina@epfl.ch; dmitry.mikulik@epfl.ch; pablo.romerogomez@epfl.ch; anna.fontcuberta-morral@epfl.ch).

N. Lassaline is with the Optical Materials Engineering Laboratory, ETH Zurich, Zürich 8092, Switzerland (e-mail: nolanl@student.ethz.ch).

Color versions of one or more of the figures in this paper are available online at http://ieeexplore.ieee.org.

Digital Object Identifier 10.1109/JSTQE.2018.2840339

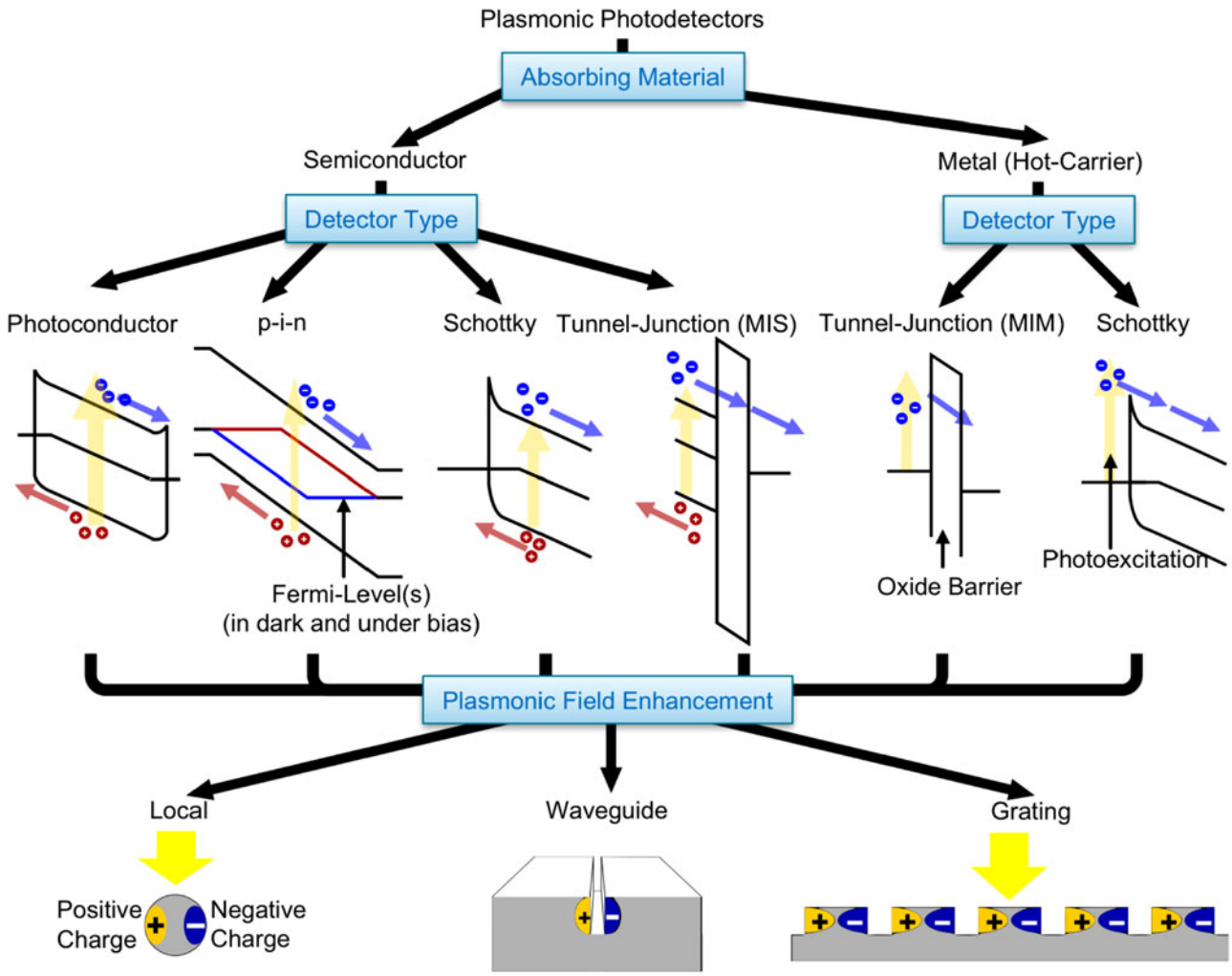

Fig. 1. Simplified classification graph of plasmonic photodetectors. The classification is organized along the "Absorbing Material" type, the "Detector Type" and the "Plasmonic Field Enhancement" type. The absorbing material typically is a semiconductor. However, lately detectors utilizing metal as an absorber are used. They are called hot-carrier photodetectors because electrons are being ejected from the metal where they were generated in a "hot" (non-thermalized) state. Among the many photodetector types we have selected four popular schemes: The tunnel-junction, p-i-n, Schottky and the photoconductor type. Any of these types can be plasmonically enhanced by a local, waveguide or grating approach.

A. Semiconductor Absorber Type Photodetectors

Among the semiconductor absorber type photodetectors the classic photoconductor is the simplest (because it introduces no inter-material borders or doping within its structure). This kind of detectors consists of an absorber placed between two contacts under external bias. The incident radiation creates additional charge carriers within the absorber increasing its conductivity, which creates the detectable photocurrent. Typically, these devices have a high dark current due to the absence of a depletion region. Yet, photoconductors can be fast detectors [36]. A much lower dark current is found in p-i-n type photodetectors. The existence of a depletion region - created by application of a reverse bias to the junction - results in a low dark current value [37]. Still, this structure is not optimal from the point of view of carrier extraction speed since a bulk charge appearing due the difference in mobility of electrons and holes limits the detector bandwidth [38], [39]. The latter is addressed by UTC (Uni-Traveling-Carrier) photodiodes that use heterostructures to make only electrons contribute to the signal current [38]–[41]. The downside of such detectors is the limited (comparing to p-i-n) thickness available for the absorption region (p-type) due to the need for electrons to diffuse out. This in turn can be addressed through a hetero-structure within the p-type region, which however makes the whole design more complicated [42]. Schottky-contacts can also be used for carrier separation. However, this commonly leads to a narrower depletion region compared to p-i-n and as a consequence higher dark currents. Lastly, oxide tunnel-junctions may be used. These ideally require high energy photons, i.e., work best for short wavelengths.

B. Hot-Carrier Type Photodetectors

Metallic absorber type detectors (or hot-carrier detectors) allow to introduce plasmonic field-enhancement in the most direct manner because they intrinsically use metals as an absorbing material. In these detectors, the strong absorption characteristics of a SPP are used to generate hot carriers. Since SPPs propagate along the surface of a metal, the hot carriers can be accumulated right at a thin oxide layer that forms a tunnel-junction or

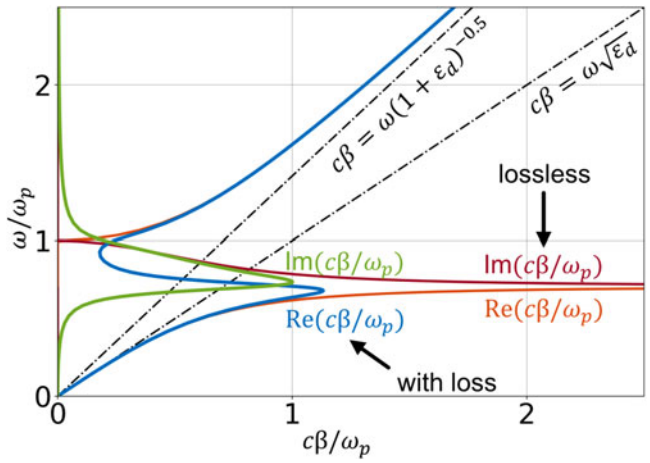

Fig. 2. Plasmon dispersion for a surface plasmon polarition on a flat border between metal with permittivity ε_m and dielectric with permittivity $\varepsilon_d = 1$. The real part of β represents the in-plane wave-vector of SPP mode and thus is inversely proportional to the mode wavelength/size ($\lambda = \frac{2\pi}{\mathrm{Re}(\beta)}$). The imaginary part of β represents propagation losses of the SPP mode, so that the propagation distance of the mode is $l = \frac{2\pi}{\mathrm{Im}(\beta)}$.

at a Schottky-contact between the metal and the semiconductor. This energy barrier is used for selecting the hot carriers and blocking off carriers in thermal equilibrium (dark current) [43]. The hot-carrier type detectors represent another ultra-fast detection scheme. The detectors however experience limitations related to the injection probability of the hot electrons from the metal to the semiconductor. This is due to the momentum mismatch and its isotropic distribution upon generation of the carriers in the metal [27], [44]. It is therefore difficult to reach high responsivities for signals at a longer wavelength.

C. Plasmonically Enhanced Detection Schemes

Each of the aforementioned detectors may be enhanced by plasmonics. Plasmonic field-enhancement takes advantage of the fact that electromagnetic field couples to charge oscillations in a metal. These hybrid charge/external field modes (plasmon polaritons) can be scaled down in size to the dimension of a charge oscillation in a metal. The size of such an oscillation can be much smaller than the corresponding light wavelength in vacuum, allowing plasmonic devices to operate at a deep-subwavelength scale. The minimal scale to which light can be confined is largely defined by the metal and is smaller (higher field-confinement) for more conductive (lower loss) metals. The concept is illustrated on Fig. 2. To plot the graphs, we used the classic equation for the SPP dispersion

$$\beta = \frac{\omega}{c}\sqrt{\frac{\varepsilon_m \varepsilon_d}{\varepsilon_m + \varepsilon_d}}, \qquad \varepsilon_m = 1 - \frac{\omega_p}{\omega^2 + i\gamma\omega},$$

where ε_d is the dielectric permittivity, ε_m is the Drude model permittivity of metal (ω_p - plasma frequency, γ - damping) and β is the propagation constant. In the case of a metal with losses we assigned $\gamma = 0.1\omega_p$.

The dispersion of a lossless plasmon would permit an infinitely large β as the frequency approaches the surface plasma frequency, which corresponds to an infinitely small SPP wavelength. In the presence of losses the SPP wavelength is still sub-diffraction limited and is smaller than a photon wavelength, yet the size is limited by the maximum value of β. The slope of the dispersion plot gives an additional information. It indicates a decrease of the group velocity as the frequency approaches the SPP resonance frequency. This effect can be exploited to enhance light-matter interaction. However, the more light is confined in the metal the lower the cross section to capture an optical signal and the higher the conductive losses. The propagation losses can be derived from the imaginary part of the dispersion plot. Thus, to utilize plasmonics efficiently an optimal point between high light-confinement and absorption as well as coupling losses to the external field needs to be found.

Local plasmonic field enhancement is commonly realized through independently acting metallic resonators or nanoparticles. In a localized plasmon an incident electromagnetic wave moves charges inside the metal that resonate with the plasmonic modes of the resonator/nanoparticle. Depending on the size and shape of such metal structures both the resonance wavelength and the field confinement can be adjusted. Because local plasmonic enhancements with metal nanoparticles are resonating independently, it is possible to deposit them directly from a solution. This allows nanoparticle type of plasmonic field-enhancement to be applied to a large variety of devices with relatively straightforward post-processing [45], [46].

In the *plasmonic waveguide enhancement approach* the light is coupled into a plasmonic waveguide such that the highest field concentration is occurring in the absorber, which also constitutes part of the waveguide. This approach allows for a better control of the plasmonic mode behavior as well as the interaction volume between the mode and an active material of the detector. However, coupling in and out of the waveguide might be required and can introduce considerable losses [47]–[49]. This type of plasmonic enhancement is most suitable when the interaction volume between light and an active material is too small for direct vertical coupling. For example, single layer graphene is a 2D-material with a uniquely tunable band gap, but it only absorbs few percent of incident light under normal illumination. In the waveguide configuration, the interaction length between waveguide mode and graphene can be tuned through the length of the graphene waveguide section. Thus, a thin layer of graphene can yield an efficient photodetector [50], [51].

The third way to implement plasmonic-field enhancement is by *plasmonic gratings* – periodic metallic structures on a surface. The grating supports plasmonic modes propagating alongside the grating. A noticeable advantage of this plasmonic enhancement type over the waveguide approach is that it does not require a separate coupling. Such detector geometries can be matched to the geometry of an optical fiber. In general grating-type plasmonic detectors are better suited for receiving the signal directly from free space than the waveguide-type due to the waveguide coupling losses.

D. Characteristics of a Detector: Noise, Quantum Efficiency, Bandwidth

Important characteristics of a photodetector are: Noise, dark current, bandwidth and quantum efficiency (QE). Knowing them and the geometrical parameters of the detector allows one to calculate other relevant quantities such as detectivity or noise equivalent power.

Noise in a photodetector has three main components: (1) Johnson-Nyquist noise created by thermal fluctuations of voltage on the load resistance, (2) shot noise occurring due to the quantum nature of the charge carriers, and (3) flicker (pink or 1/*f*) noise whose spectrum power density is roughly inversely proportional to the frequency. Important to note that depending on the specific structure of a detector other noise components can be present such as the short channel excess noise in the field effect transistor [52], [53]. The Johnson-Nyquist noise is described by the variance

$$\left\langle J_{th}^2 \right\rangle = \frac{4k_B T}{R_L}\Delta\nu,$$

where R_L is the external load and $\Delta\nu$ is the detector bandwidth, k_B is the Boltzmann constant and T is the temperature. This noise is affecting the current that is measured on the load but is external to the detector itself. The shot noise occurs due to the fact that current flow is not continuous but consists of a large number of elementary charges carried by charged particles. Assuming Poisson statistics for the arrival of such carriers at respective contacts one can obtain:

$$\left\langle J_{sh}^2 \right\rangle = 2\mathrm{e}\left(J_s + J_d\right)\Delta\nu,$$

where J_s is the corresponding photodetector current that is creating the noise. Shot noise in photodetectors has two components: Signal J_s and dark current noise J_d. This noise is particularly problematic for detectors with low QEs and high dark currents. The flicker noise or 1/*f* noise is created by local oscillations in a conductor and depends on such things as the number of carriers or their mobility. It is relevant at lower frequencies.

The *dark current* has three main components for the detector types listed in Fig. 1: Semiconductor dark current, Schottky-barrier dark current and tunneling-junction dark current. The semiconductor dark current can be described by

$$J_{d,sem} = S\mathrm{e}E\left(\mu_e N_C e^{-\frac{W_C - W_{fe}}{kT}} + \mu_h N_V e^{-\frac{W_{fh} - W_V}{kT}}\right),$$

where S is a cross-section through which the current flows, E is the applied electric field, $\mu_{e,h}$ are carrier mobilities, $W_{C,V,fe,fh}$ are the energies of conduction band, valence band, quasi-Fermi-level of electrons, quasi-Fermi-level of holes and $N_{C,V}$ are the effective densities of states in the bands. The quasi-Fermi levels depend on the offset bias and respective carrier densities. The $J_{d,sem}$ is directly proportional to the carrier densities and is high for photoconductors whereas it is low in p-i-n photodiodes. The Schottky-barrier dark current can be calculated as follows [43]:

$$J_{d,SB} = SA_G T^2 e^{-\frac{\mathrm{e}\phi}{kT}}\left(e^{\frac{\mathrm{e}V}{kT}} - 1\right),$$

where ϕ is the height of the Schottky-barrier (in Volts), V is the bias applied across the junction and A_G is the Richardson constant [54]. This current component is dominant in hot-carrier Schottky detectors due to their low QE. The tunneling current through a potential barrier can be calculated through the Wentzel-Kramers-Brillouin approximation for the Schrodinger equation and for low electron energies (comparing to the barrier height) it is roughly proportional to the square of applied voltage [55]

$$J_{tunn} = CV^2,$$

where C is a constant. Similar to the Schottky-barrier dark current this type of dark current is often dominant in the hot-carrier type detectors due to a low QE.

The *photocurrent* I_s of a signal generated by an incident signal P_s directly depends on the quantum efficiency (QE).

$$I_{s,d} = QE \cdot \frac{e}{\hbar\omega}P_s = \eta_a\eta_i,$$

where e is the elementary charge and $\hbar\omega$ the photon energy. The *QE* of a detector is given by

$$QE = \frac{\#Photons\ absorbed}{\#Photons\ incident} \cdot \frac{\#Charges\ extracted}{\#Photons\ absorbed} = \eta_a\eta_i$$

It can thus be organized around two terms: (1) The absorption efficiency η_a and (2) the internal quantum efficiency η_i. The absorption efficiency can be derived from the exponential dependence of the light intensity on the propagation length l

$$I = I_0 e^{-\alpha l},$$

where α is the absorption coefficient. So for the absorption efficiency we have: $\eta_a = (1-R)\cdot(1-e^{-\alpha l})$ where *R* is the reflectivity. The internal quantum efficiency accounts for the finite life-time and velocity of carriers that lead to loss of carriers that no longer contribute to the detector current. So ideally a detector should be long enough to absorb most of the incident light but not too long to avoid loss of carriers. Worth to note that to increase the internal quantum efficiency additional gain mechanisms can be introduced such as avalanche multiplication [56] and photoconductive gain [57].

The *3 dB frequency response* or *bandwidth* of a photodiode also depends on the length. On the one hand a short length provides the fastest carrier extraction time that should result in a high bandwidth. On the other hand the short length increase the capacitance of the photodetector which limits the bandwidth. To illustrate how the bandwidth of a detector depends on its properties let's consider a simple model: A device with an absorber thickness d, with carrier extraction time $\tau_e = \frac{1}{v_e}d$ (v_e is the carrier velocity under the given bias), recombination time τ_r and capacitive discharge time $\tau_{RC} = RC = R\varepsilon A_{RC}d^{-1}$ (assuming a plate capacitor of area A_{RC} with a dielectric of permittivity ε). In this model the impulse response of the device can be approximated by a multiplication of the impulse responses of the carrier extraction and recombination that needs to be convoluted with the impulse response of the capacitive discharge

$$h\left(t\right) = \left(h_e\left(t\right)\cdot h_r\left(t\right)\right) * h_{RC}\left(t\right),$$

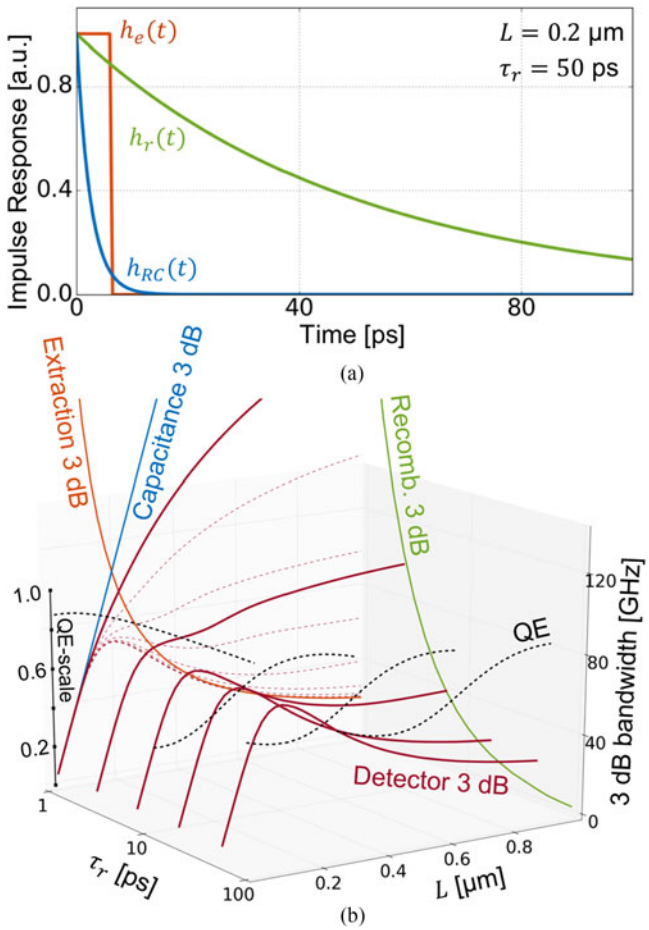

Fig. 3. (a) Impulse responses of carrier extraction, recombination and capacitor (d - absorber thickness, τ_r - recombination time). (b) 3 db bandwidth for the full device (red), extraction time (orange), recombination time (green), capacitor (blue). QE-scale is shown on the right side. QE drops down with decreasing recombination time.

where $h_e(t)$ is a rectangular-shaped function with the values 1 for $t \in [0, \tau_e]$ and 0 otherwise, h_r is an exponential decay function with the time constant τ_r. Likewise, h_{RC} is an exponential decay with time constant τ_{RC}. In the frequency domain multiplications become convolutions and vice-versa

$$H(\omega) = (H_e(\omega) * H_r(\omega)) \cdot H_{RC}(\omega).$$

The dependence of the 3 dB bandwidth of the corresponding model parameters is shown in Fig. 3. For the modeling we used $\nu_e \approx 3 \cdot 10^6 \cdot$ cm/s, $\varepsilon A_{RC} \approx 10 \cdot$ pF $\cdot$ nm and $R = 50\ \Omega$. One can see that at small absorber thickness d the bandwidth is defined by the capacitor response whereas for large d it depends on the carrier recombination time. If the recombination is slow, most of the carriers can reach corresponding contacts – then the bandwidth has an optimum in relation to the device thickness defined by the optimal point between extraction time and capacitor time constant. If the recombination is fast the carriers from far ends of the device will never reach their contacts providing higher bandwidth. However, in this case, the ratio of extracted carriers and therefore the internal quantum efficiency goes down.

TABLE I
DETECTOR TYPES PROS & CONS

Type	QE	Bandwidth	Noise	Dark Current
Photoconductive	-+	+	--	--
p-i-n	++	+-	++	++
Schottky	-+	+	-+	-+
Tunnel-Junction	+-	+-	+-	+-
Hot-Carrier	--	++	--	--

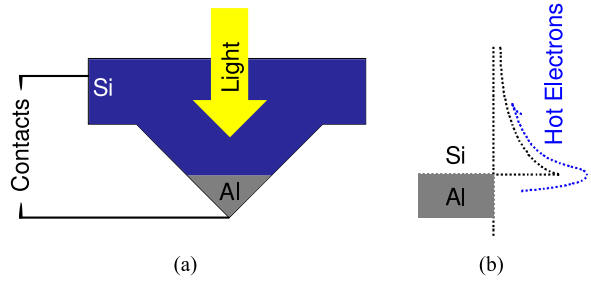

Fig. 4. (a) Schematic illustration of plasmonically enhanced hot-carrier Shottky-photodetector on silicon. The light is passing through the silicon substrate and is being enhanced on the tip of a reversed pyramid covered by a layer of aluminum. (b) Schematic illustration of corresponding band structure and hot-carrier injection. The detector shown was designed to function at room temperature for wavelengths around 2.5 μm. (See [43], [60].).

An attempt to sum up the section is presented in Table I. The table marks each property by "–","-+","+-","+" and "++" in order from poor- to good-performance. It should be noted, that the table is only marking the commonly occurring properties of photodetectors. There are always schemes that under- and over-perform with respect to what is expected.

In the following sections, we will elucidate the three types of plasmonic field enhancements to improve photodetection.

III. IMPLEMENTATION EXAMPLES OF PLASMONIC DETECTORS

Subsequently, we elucidate the plasmonic concepts by discussing different detection types. We have organized the different implementation schemes along the three field enhancement schemes discussed above.

A. *Localized Plasmonic Field Enhancement Photodetectors*

Localized plasmonic enhancement can be used in multiple ways to enhance photodetection.

In a first example the localized plasmonic enhancement is used to build a cheap mid-IR detector on silicon. Normally, mid-IR detectors involve exotic materials [58], [59]. However, by resorting to a hot-carrier Schottky type detector one should be able to detect mid-IR light even at a silicon-Al interface. This would make them suitable for large scale production in silicon. Yet, hot carrier type detectors tend to have high dark current for longer wavelengths. In Fig. 4, this is solved by minimizing the Schottky-contact area while maintaining a high level of light absorption by means of a localized plasmonic field enhancement [43], [60]. In more detail, Fig. 4(a) shows the schematic of the basic element of a photodetector for wavelength of 2.5 μm - a silicon pyramid with an Al-covered tip. The detector concentrates light that passes through a silicon wafer along an

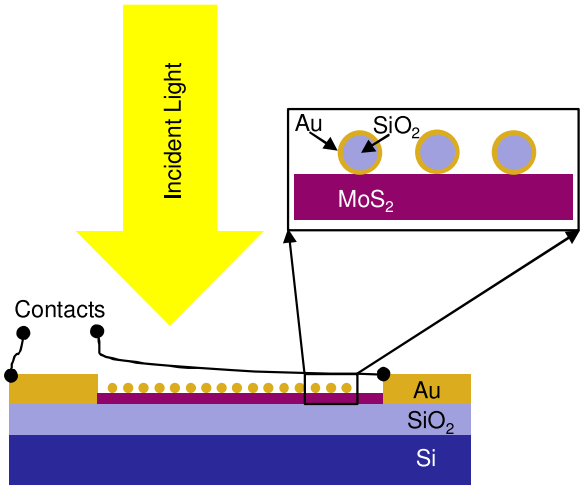

Fig. 5. Schematic illustration of a MoS_2 monolayer photoconductive photodetector plasmonically enhanced by dispersed Au nanoparticles. With surface density of less than 1% the nanoparticles yield threefold enhancement in the photocurrent. (See [63]).

aluminum-covered tip of the pyramid, so that localized plasmon resonances are excited at the Al-Si interface. Hot-carriers generated in the Al are then being injected into the Si through the Schottky-barrier creating a photocurrent, Fig. 4(b). It was shown that there is an optimum value for the Schottky-barrier height which provides the best trade-off between injection of carriers through the barrier and the dark-current noise (in terms of signal-to-noise ratio) [43]. The authors of this work reported on a responsivity of 0.1 mA/W, which is not large but new for a mid-IR detector in this material system.

In the next example, localized plasmonic enhancement is employed to increase the absorption efficiency of emerging 2D materials which, due to advancement in production technology, recently gained considerable attention in the field of photodetectors [25], [61], [62]. 2D materials are attractive as they give access to materials with new bandgaps and other interesting characteristics. Yet, a single monolayer by itself is not sufficient to absorb enough light to make an efficient detector which makes it necessary to enhance the absorption. In the example of Fig. 5 the field was enhanced in the vicinity of the absorbing monolayer by dispersing core-shell Si-Au nanoparticles [63]. The detector itself acts as a photoconductor, where the single crystal monolayer of MoS_2 is the conducting absorber. MoS_2 was chosen as its direct band gap can be tuned from the visible to the UV range [64]–[66]. The monolayer of MoS_2 was produced using a chemical vapor deposition technique that opens up commercial application possibilities for the technology. The nanoparticles were deposited through a solution process on top of a ready device with surface density of less than 1%, and yielded a threefold enhancement in the photocurrent (to around 0.8 mA/W at wavelength of 630 nm). A significant role in the responsivity enhancement was played by the tunability of the plasmonic resonance frequency of nanoparticles that can be adjusted to the absorption of the monolayer [67].

In the same way that localized plasmonic enhancement was applied to monolayer materials the technique can be used on

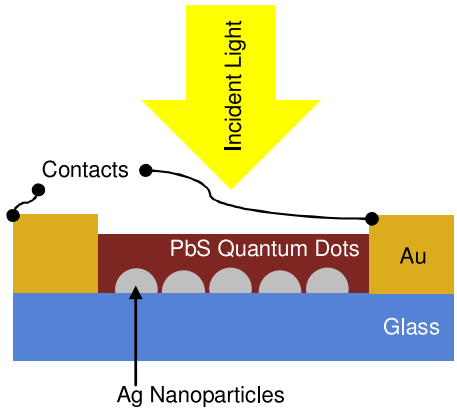

Fig. 6. Schematic illustration of a QD-photodetctor enhanced by plasmonic Ag nanoparticles beneath the QD-film. At wavelength of 1 μm the detector showed a responsivity of 300 A/W (See [68]).

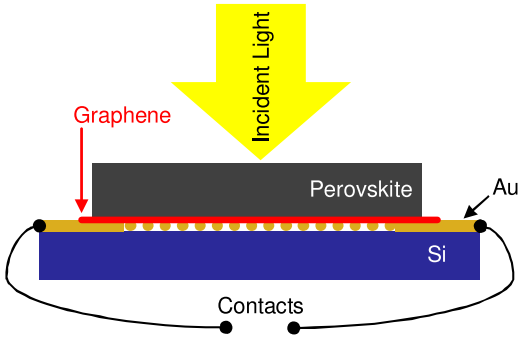

Fig. 7. Schematic illustration of a hybrid perovskite/graphene photodetector with plasmonic enhancement. The enhancement comes from Au nanoparticles dispersed beneath the graphene layer. At a wavelength of 0.5 μm the detector showed responsivity of 2000 A/W (See [71]).

quantum-dot (QD) structures [68]. QD-based detectors are attractive because they can be fabricated with a simple deposition technique and because they offer a possibility to tune the band gap across a wide spectral range between the infrared and the visible. Yet, the absorption coefficient of QD films is not sufficient to absorb all the incident light within a thin QD layer. A thin layer however, is needed to keep the dark current of the photoconductive detector reasonably low. In addition, a thin layer can also be advantageous to efficiently extract carriers within the carrier life-time given the low mobility of the QD films [68], [69]. Fig. 6 shows such a detector based on a few hundred nm thick film of colloidal quantum dots. The reported results showed that the photoresponse of the studied QD photodetector can be increased more than twofold by the application of Ag nanoparticles on the back side of the QD-film [68]. The responsivity shown is around 300 A/W at a wavelength of 1 μm.

Recently, photo-conductive gains in the order of 10^8 were reported in hybrid graphene-absorber stacks [57]. It would thus be interesting to apply the concept to a large variety of materials. In particular to materials where the carrier lifetime and mobility require a thin absorber layer. Fig. 7 shows an example of such a hybrid graphene-perovskite photoconductive detector. Perovskites have become popular absorbers because

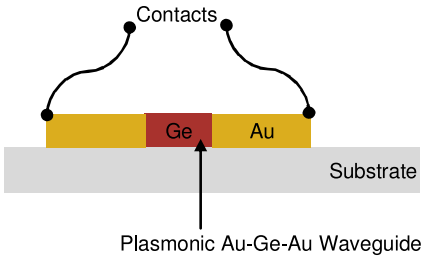

Fig. 8. Schematic illustration of a plasmonic waveguide photoconductive Ge detector on Si/SiO_2 substrate. The photodetector has a frequency response beyond 100 GHz and offers a responsivity of 0.38 A/W. (See [73], [74]).

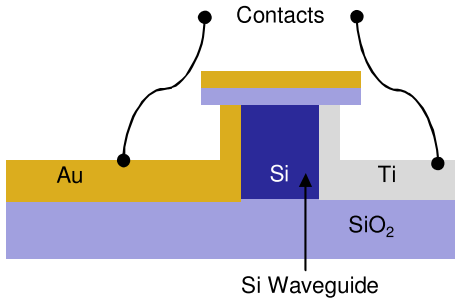

Fig. 9. Schematic illustration of a plasmonic hot-carrier Schottky waveguide photodetector on silicon. The detector demonstrated a responsivity of 0.12 A/W and a bandwidth of 40 GHz. (See [28]).

they are easy to deposit and showed high efficiency in the field of photovoltaics. They offer a high carrier-lifetime but suffer from a modest carrier mobility [70]. The carriers have thus to be extracted within a thin layer close to the graphene conductive layer. By applying dispersed plasmonic particles below the graphene layer the electromagnetic field is enhanced near the graphene perovskite border, promoting a fast carrier extraction [71]. Once the carriers have reached the graphene, they benefit from the high carrier mobility yielding a large photoconductive gain [57], [72]. In the scheme reported in [71], Fig. 7, the additional plasmonic enhancement in form of Au nanoparticles located beneath the graphene layer were shown to both increase the detector photocurrent (by around 2 times, up to $2 \cdot 10^3$ A/ W under a 10 V bias) and its response speed (signal rise time in the order of 1.5 s) at a wavelength around 500 nm. The latter is due to the proximity of the nanoparticles to the graphene layer, which boosts the absorption in a region with the shortest carrier extraction time.

B. Plasmonically Enhanced Waveguide Photodetectors

Waveguide type photodetectors are important components for on-chip optical communication because they can be monolithically integrated with electronics. Typical example of waveguides used to guide light on a silicon chip are rectangular silicon strips placed on an oxide layer. At the terminal end of such a waveguide one could place a photodetector. The photodetector is then an extension of the waveguide that comprises one of the aforementioned photo detection schemes. Waveguide photodetectors can also be used to detect signals from an optical fiber or free space, but that requires additional light coupling.

Optical communications rely on ultra-fast detectors with a high responsivity. A plasmonic waveguide field enhanced photoconductive detector is depicted in Fig. 8, [73], [74]. Here, a symmetric metal-semiconductor-metal waveguide has been used to enhance the field in the slot between the two metals. The MIM plasmonic waveguide allows to confine the field in a narrow region, and thus decreases the absorber volume and accelerate the carrier extraction. Due to the simple photoconductive structure the detector is producible on a silicon substrate (Ge strips is deposited directly on top of two Au lines/contacts forming the waveguide/detector). The detector was demonstrated to have a bandwidth beyond 100 GHz with responsivity of 0.38 A/W. It works in the absorption band of Germanium at 1.3 μm.

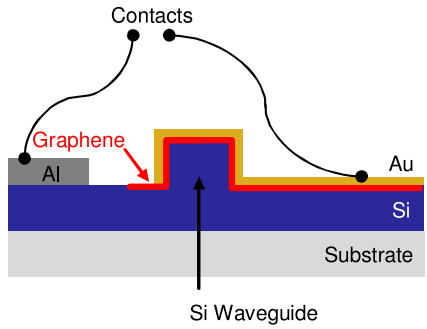

Fig. 10. Schematic illustration of a plasmonic enhanced graphene photodetector. Upon reverse biasing a responsitivtiy of 0.37 A/W was measured at wavelength of 1.55 μm. (See [75]).

Another ultra-fast photodetector approach relies on hot-carrier photodetection [16], [27]. An optical communication implementation is depicted in Fig. 9 [28]. It shows a MIM plasmonic waveguide. The concept exploits the hot-carrier injection in the metallic waveguides across the Schottky junction formed by the silicon waveguide in the center and the titanium contact. The plasmonic absorption and hot-carrier injection across the 75 nm wide dielectric layer guarantees a fast speed. A bandwidth of 40 GHz and a responsivity of 0.12 A/W at 1.55 μm was found when applying a bias voltage of 3.5 V.

Recently, graphen is increasingly used for photo detection. An approach for a plasmonic hot-carrier waveguide photodetector on silicon for the wavelength of 1.55 μm suggests to utilize a metal-graphene-semiconductor stack to improve the efficiency of the internal-photoemission [75]. The detector is depicted in Fig. 10. In a latter publication [44] the role of graphene was explained in more detail. The authors show that the scheme allows to enhance the efficiency of the internal photoemission due to a prolonged carrier life-time in the graphene layer (comparing to near-interface life-time without graphene), which increases the possibility for carriers to be injected into silicon. The detector reached a responsivity of 0.085 A/W at 1.55 μm telecom wavelength. In another experiment - by reverse biasing the detector - an avalanche photo multiplication effect was exploited leading to a responsivity of 0.37 A/W at a wavelength 1.55 μm [75].

Most recently, new graphen photodetectors relying on a bolometric thermal effect have emerged [76] and [77]. The plasmon-

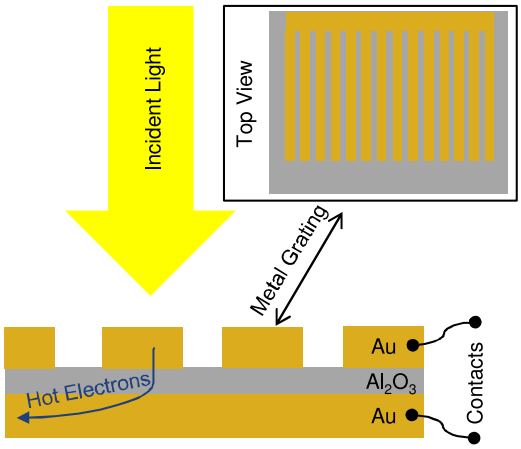

Fig. 11. Schematic illustration of a MIM hot-carrier plasmonic photodetector for the visible to ultraviolet frequency range. The hot carriers generated in the top metal grating are tunneling through a thin oxide layer creating a photocurrent. (See [35]).

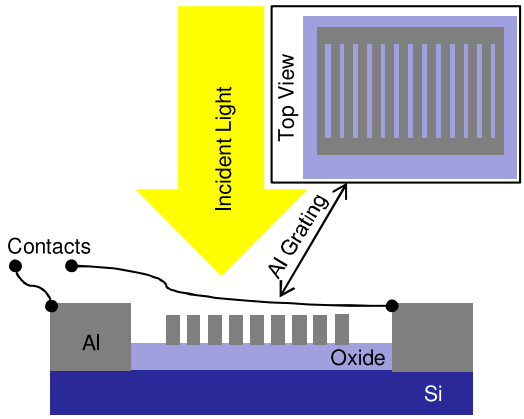

Fig. 12. Schematic illustration of plasmonically enhanced photoconductive detector on silicon. Due to the charge accumulation at the Shottky-contacts between Al and Si, the photodetector also provides photocurrent gain. A responsivity of 10 A/W at wavelength of 400 nm was reported. (See [78]).

ically enhanced detectors have demonstrated operation at 100 Gbit/s with responsivities of 0.5 A/W at 1.55 μm [77].

C. Plasmonically Enhanced Grating Photodetectors

Plasmonic gratings are periodic metallic structures that support plasmonic modes propagating alongside its surface. Such gratings can be used simultaneously as color-filters, electrical-contacts and for field enhancement.

MIM hot-carrier tunneling photodetectors are among the simplest detectors one can imagine. They can be fabricated by thin-film deposition, which makes them compatible with multiple different technologies. The responsivity of MIM detectors is however very low. To address the low responsivity utilization of plasmonic grating field enhancement was suggested, see Fig. 11, [35]. The detector in Fig. 11 shows a plasmonic grating providing a highly concentrated field close to the oxide layer, which enhances the hot-electron emission and therefore leads to a higher tunneling photocurrent. The detector was shown to work at around a 400 nm wavelength with a responsivity reaching 0.25 mA/W. This is still a low responsivity, but it also represents one of the most simple detector schemes.

A detector with a similar plasmonic grating to enhance the field of a photoconductive silicon detector is depicted in Fig. 12, see [78]. The detector exploits the efficient absorption of 400 nm UV light in silicon. Light is then detected by means of the photoconductive effect across the Al contacts. The detector utilizes Al as plasmonic grating material, which possesses good optical properties up to ultraviolet frequency range, and it also makes the structure CMOS-compatible, which is important for large-scale commercial applications [79]. A Schottky-junction forms between the Al-Si contacts at the edge. This provides a carrier accumulation effect that reduces the height of the barrier resulting in a photocurrent gain at lower signal rates (below 10 GHz). With the photocurrent gain, the detector was measured to have responsivity values above 10 A/W at optical frequencies around 400 nm.

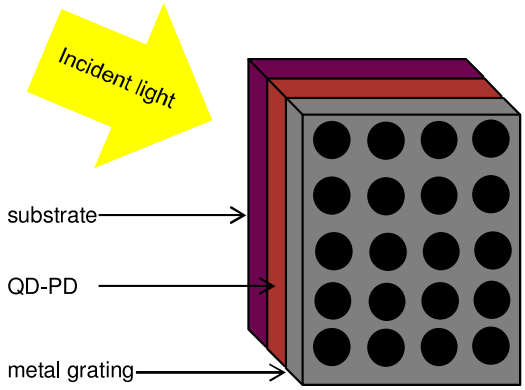

Fig. 13. Schematic illustration of heterostructure QD-photodetector enhaced by a plasmonic grating attached to the back-side. The illimunation is coming from the substrate side. The detector reached responsivity of 1 A/W at wavelength of 8 μm (See [80]).

To access new spectral wavelengths, it is most attractive to use quantum dots (QDs) that are engineered to absorb at a particular wavelength. A heterostructure photodetector with a multilayer of QDs and a plasmonic grating for field enhancement is shown in Fig. 13, see [80]. The grating was attached to one side of the QD layers. A resonant enhancement of the photodetector absorption due to the plasmonic grating by a factor 2 was found experimentally. A responsivity of 1 A/W for light at 8 μm was reported. More recently, an infrared camera was demonstrated with this type of detector [81].

IV. A Nanowire Array Plasmonic Photodetector

In the previous sections, we have shown a large variety of detectors where plasmonics has been used to enhance the responsivity or where plasmonics has been utilized to reach ultra-high operation speed. However, the ultimate photodetector should feature a combination of the following:

- A high responsivity (on the order of 1 A/W)
- A small footprint (a few μm^2)

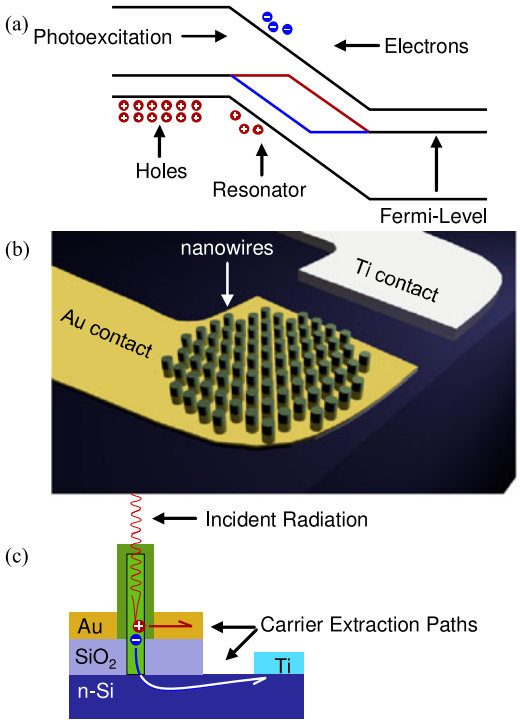

Fig. 14. (a) Schematic illustration of the photodetector working principle: electrons and holes are generated within a standard p-i-n structure. However by means of light management the absoprtion is shifted towards the p-side yielding UTC-like performance. (b) Scheme of the nanowire array photodiode with assymetric carrier extraction paths: geometry on the nanowires provide assimetric extraction paths for electrons and holes compensating for their mobility difference.

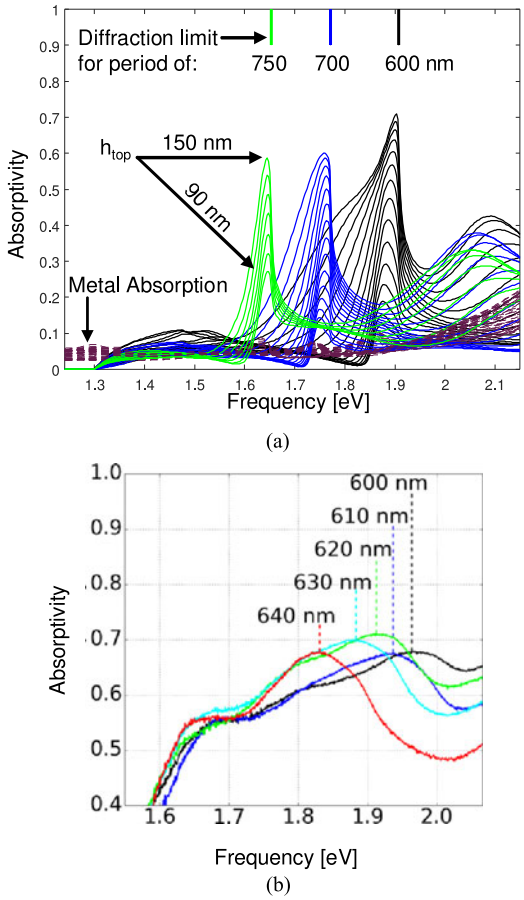

Fig. 15. (a) Spectra calculated for nanowire arrays of different periodicities (period Λ is shown on the graph) and heights of nanowire segments above the gold contact (denoted as h_{top}). (b) Measured spectra of absorption of GaAs naowire arrays grown on GaAs substrate and covered by 50 nm of gold through a directional e-beam evaporation (period of each structure is marked by a dashed line).

- Highest speed (>100 GHz)
- A low dark current
- Offer CMOS compatible fabrication
- A high input power dynamic range

Unfortunately – and despite of all efforts – such a photodetector is still at large.

In this section, we would like to look beyond of the current technologies and introduce a visionary detector that combines the field enhancement of plasmonics, the low dark-current of a p-i-n structure, the high-speed of a UTC photodiode and offers a silicon compatible growth of the emerging field of III-V nanowires.

The operation scheme of the detector is depicted in Fig. 14(a). The detector mainly comprises of a classical p-i-n structure offering a low dark current. To reach high-speed performance a resonator (in the form of a plasmonic structure) is introduced to force the absorption close to the p-contact. This provides a short drift path for the holes – similar to a UTC photodiode.

An implementation of the concept is suggested in Fig. 14(b) and (c). The detector consists of an absorber in the form of a III/V nanowire array. The array is sticking out of a gold contact, which is separated from the substrate by an oxide layer. From the bottom side the nanowires are contacted through n-type Si to the titanium contact.

The detector offers a unique combination of advantages. First, it features UTC-like performance. This is realized by a core-shell nanowire structure that extracts the electrons along the wire to the n-type Si substrate whereas the holes are only moving laterally to the nanowire-shell. The short path of the holes with the lower mobility offers the speed-advantage of the UTC concept. Second, the p-i-n structure featuring a low dark current is formed by a p-type shell, an intrinsic core and a n-type substrate. Third, high responsivity is reached due to the gold contact that also acts as a plasmonic grating to enhance the field within the nanowires and that prevents the light from leaking into the substrate [82]–[84]. Forth, the small dimensions of the nanowires allow to utilize high-quality III-V materials on silicon which are known for the high detection performance. Last but not least, III-V nanowires can be directly grown on a silicon substrate with a minimal amount of structural defects due to a small footprint and fast strain relaxation [85]–[88]. Therefore, our detector will be compatible with the silicon platform.

To analyze the absorption of the photodetector we performed several sets of simulations varying the structural parameters. Fig. 15(a) shows a representative set. The simulations were performed for array periods equal to 650, 700 and 750 nm and nanowire heights above the contact layer (gold) from 90 to 150 nm. The rest of the parameters were: gold thickness

−50 nm, total nanowire height −250 nm, nanowire shell radius −120 nm, nanowire core radius −100 nm. Absorption is divided into two parts: Absorption in GaAs (shown in different colors for different structure periods) and absorption in the gold contact (shown as dashed lines for all simulations).

One can see from Fig. 15(a) that the absorption in the metal contact is close to negligible in all cases, so it is not considered as an issue. Absorption in GaAs exhibits a sharp peak close to the diffraction limit, which increases along with the increase of the nanowire height above the gold contact. The dependence of the absorption on the structure period (equal to the diffraction limit in the air surroundings) indicates the presence of laterally propagating modes within the top layer of the detector (above the gold contact). The width of the absorption peak is relatively narrow, and its central frequency can be tuned in a wide spectral range by changing the periodicity of the nanowire array.

Carrier-dynamics simulations of the detector predict a 180 GHz bandwidth and a 0.3 A/W responsivity at around 750 nm wavelength as well as a tunability in the optical frequency range.

To test the resonant behavior of the nanowire array we have fabricated a wafer with arrays of GaAs nanowires grown on a (111) GaAs substrate by selective area growth [89], [90]. Fig. 15(b) shows the absorption measurements of the fabricated array. The position of the absorption peak follows the prediction of the simulations while the resonance shape is deviating due to the imperfections of the fabricated array. It is however evident that laterally propagating modes predicted by the simulation are present in the structure. In a next step of the development the full detector structure may be realized on a silicon wafer.

V. Conclusion

We have shown in our review that plasmonics is an attractive technique to enhance the responsivity of detectors that normally would not be efficient because they rely on thin absorbers (such as 2D-materials or thin QD-films) or because they operate at a wavelength where absorption is inefficient. Along the same lines, we have shown many examples where plasmonics has allowed to shrink the device footprint, which is of high interest in e.g., an expensive CMOS technology. Lastly, we have also commented on first experiments that show ultra-fast responses indicating that plasmonic concepts might offer a new path towards compact high-speed detectors.

Finally, we have suggested a new scheme of a plasmonically enhanced III-V nanowire array on silicon detector. The detector potentially features the low dark current and high responsivity of a p-i-n structure, the high-speed of a UTC photodiode combined with the high crystalline quality and silicon compatibility of III-V nanowires. It was predicted through numerical simulation to reach 180 GHz bandwidth with responsivity of 0.3 A/W at optical wavelengths (600–800 nm).

References

[1] S. A. Maier *et al.*, "Plasmonics—A route to nanoscale optical devices," *Adv. Mater.*, vol. 13, no. 19, Oct. 2001, pp. 1501–1505.

[2] H. A. Atwater and A. Polman, "Plasmonics for improved photovoltaic devices," *Nature Mater.*, vol. 9, no. 3, pp. 205–213, Mar. 2010.

[3] J. A. Schuller *et al.*, "Plasmonics for extreme light concentration and manipulation," *Nature Mater.*, vol. 9, no. 3, pp. 193–204, Mar. 2010.

[4] D. K. Gramotnev and S. I. Bozhevolnyi, "Plasmonics beyond the diffraction limit," *Nature Photon.*, vol. 4, no. 2, pp. 83–91, Feb. 2010.

[5] M. Kauranen and A. V. Zayats, "Nonlinear plasmonics," *Nature Photon.*, vol. 6, no. 11, pp. 737–748, Nov. 2012.

[6] J. Leuthold *et al.*, "Plasmonic communications: Light on a wire," vol. 24, no. 5, pp. 28–35, 2013.

[7] C. Haffner *et al.*, "All-plasmonic Mach-Zehnder modulator enabling optical high-speed communication at the microscale," *Nature Photon.*, vol. 9, no. 8, pp. 525–528, Aug. 2015.

[8] M. L. Brongersma, "Plasmonic photodetectors, photovoltaics, and hot-electron devices," *Proc. IEEE*, vol. 104, no. 12, pp. 2349–2361, Dec. 2016.

[9] E. Ozbay, "Plasmonics: Merging photonics and electronics at nanoscale dimensions," *Science*, vol. 311, no. 5758, pp. 189–193, Jan. 2006.

[10] C. Hoessbacher *et al.*, "Optical interconnect solution with plasmonic modulator and ge photodetector array," *IEEE Photon. Technol. Lett.*, vol. 29, no. 21, pp. 1760–1763, Nov. 2017.

[11] M. L. Brongersma, N. J. Halas, and P. Nordlander, "Plasmon-induced hot carrier science and technology," *Nature Nanotechnol.*, vol. 10, no. 1, pp. 25–34, Jan. 2015.

[12] W. Heni *et al.*, "108 Gbit/s plasmonic Mach-Zehnder modulator with >70-GHz electrical bandwidth," *J. Lightw. Technol.*, vol. 34, no. 2, pp. 393–400, Jan. 2016.

[13] C. Hoessbacher *et al.*, "Plasmonic modulator with >170 GHz bandwidth demonstrated at 100 GBd NRZ," *Opt. Express*, vol. 25, no. 3, pp. 1762–1768, Feb. 2017.

[14] 2016. [Online]. Available: http://www.ethernetalliance.org/roadmap/

[15] H. Mikami, L. Gao, and K. Goda, "Ultrafast optical imaging technology: Principles and applications of emerging methods," *Nanophotonics*, vol. 5, pp. 441–453, 2016.

[16] M. W. Knight, H. Sobhani, P. Nordlander, and N. J. Halas, "Photodetection with active optical antennas," *Science*, vol. 332, no. 6030, pp. 702–704, May 2011.

[17] M. W. Knight *et al.*, "Embedding plasmonic nanostructure diodes enhances hot electron emission," *Nano Lett.*, vol. 13, no. 4, pp. 1687–1692, Apr. 2013.

[18] W. Zhang *et al.*, "High-performance AlGaN metal-semiconductor-metal solar-blind ultraviolet photodetectors by localized surface plasmon enhancement," *Appl. Phys. Lett.*, vol. 106, no. 2, Jan. 2015.

[19] Y. Salamin *et al.*, "Direct conversion of free space millimeter waves to optical domain by plasmonic modulator antenna," *Nano Lett.*, vol. 15, no. 12, pp. 8342–8346, Dec. 2015.

[20] W. L. Barnes, A. Dereux, and T. W. Ebbesen, "Surface plasmon subwavelength optics," *Nature*, vol. 424, no. 6950, pp. 824–830, Aug. 2003.

[21] A. Sobhani *et al.*, "Narrowband photodetection in the near-infrared with a plasmon-induced hot electron device," *Nature Commun.*, vol. 4, Mar. 2013, Art. no. 1643.

[22] P. Berini and I. De Leon, "Surface plasmon-polariton amplifiers and lasers," *Nature Photon.*, vol. 6, no. 1, pp. 16–24, Jan. 2012.

[23] E. Bermudez-Urena *et al.*, "Plasmonic waveguide-integrated nanowire laser," *Nano Lett.*, vol. 17, no. 2, pp. 747–754, Feb. 2017.

[24] T. J. Echtermeyer *et al.*, "Strong plasmonic enhancement of photovoltage in graphene," *Nature Commun.*, vol. 2, Aug. 2011, Art. no. 458.

[25] A. N. Grigorenko, M. Polini, and K. S. Novoselov, "Graphene plasmonics," *Nature Photon.*, vol. 6, no. 11, pp. 749–758, Nov. 2012.

[26] J. D. Lin, H. Li, H. Zhang, and W. Chen, "Plasmonic enhancement of photocurrent in MoS_2 field-effect-transistor," *Appl. Phys. Lett.*, vol. 102, no. 20, May 2013, Art. no. 203109.

[27] I. Goykhman, B. Desiatov, J. Khurgin, J. Shappir, and U. Levy, "Waveguide based compact silicon Schottky photodetector with enhanced responsivity in the telecom spectral band," *Opt. Express*, vol. 20, no. 27, pp. 28594–28602, Dec. 2012.

[28] S. Muehlbrandt *et al.*, "Silicon-plasmonic internal-photoemission detector for 40 Gbit/s data reception," *Optica*, vol. 3, no. 7, pp. 741–747, Jul. 2016.

[29] A. Casadei *et al.*, "Polarization response of nanowires a la carte," *Sci. Rep.*, vol. 5, Jan. 2015, Art. no. 7651.

[30] Y. L. Jing *et al.*, "Pixel-level plasmonic microcavity infrared photodetector," *Sci. Rep.*, vol. 6, May 2016, Art. no. 25849.

[31] E. Panchenko, J. J. Cadusch, T. D. James, and A. Roberts, "Plasmonic metasurface-enabled differential photodetectors for broadband optical polarization characterization," *Acs Photon.*, vol. 3, no. 10, pp. 1833–1839, Oct. 2016.

[32] S. Qu, C. C. Ma, and H. X. Liu, "Tunable graphene-based hybrid plasmonic modulators for subwavelength confinement," *Sci. Rep.*, vol. 7, Jul. 2017, Art. no. 5190.

[33] M. Ayata *et al.*, "High-speed plasmonic modulator in a single metal layer," *Science*, vol. 358, no. 6363, pp. 630–632, Nov. 2017.

[34] F. M. Wang and N. A. Melosh, "Plasmonic energy collection through hot carrier extraction," *Nano Lett.*, vol. 11, no. 12, pp. 5426–5430, Dec. 2011.

[35] H. Chalabi, D. Schoen, and M. L. Brongersma, "Hot-electron photodetection with a plasmonic nanostripe antenna," *Nano Lett.*, vol. 14, no. 3, pp. 1374–1380, Mar. 2014.

[36] S. Y. Chou and M. Y. Liu, "Nanoscale tera-hertz metal-semiconductor-metal photodetectors," *IEEE J. Quantum Electron.*, vol. 28, no. 10, pp. 2358–2368, Oct. 1992.

[37] C. T. DeRose *et al.*, "Ultra compact 45 GHz CMOS compatible Germanium waveguide photodiode with low dark current," *Opt. Express*, vol. 19, no. 25, pp. 24897–24904, Dec. 2011.

[38] T. Ishibashi, S. Kodama, N. Shimizu, and T. Furuta, "High-speed response of uni-traveling-carrier photodiodes," *Jpn J. Appl. Phys. Part 1, Regul. Papers Brief Commun. Rev. Papers*, vol. 36, no. 10, pp. 6263–6268, Oct. 1997.

[39] C. Li *et al.*, "High-responsivity vertical-illumination Si/Ge uni-traveling-carrier photodiodes based on silicon-on-insulator substrate," *Sci. Rep.*, vol. 6, Jun. 2016, Art. no. 27743.

[40] T. Ishibashi *et al.*, "Uni-traveling-carrier photodiodes," in *Proc. OSA Trends Opt. Photon.*, vol. 13, 1997, pp. 83–87.

[41] N. Shimizu, N. Watanabe, T. Furuta, and T. Ishibashi, "InP-InGaAs uni-traveling-carrier photodiode with improved 3-dB bandwidth of over 150 GHz," *IEEE Photon. Technol. Lett.*, vol. 10, no. 3, pp. 412–414, Mar. 1998.

[42] J. Li *et al.*, "Ultrafast dual-drifting layer uni-traveling carrier photodiode with high saturation current," *Opt. Express*, vol. 24, no. 8, pp. 8420–8428, Apr. 2016.

[43] M. Grajower *et al.*, "Optimization and experimental demonstration of plasmonic enhanced internal photoemission silicon schottky detectors in the Mid-IR," *ACS Photon.*, vol. 4, no. 4, pp. 1015–1020, Apr. 2017.

[44] U. Levy, M. Grajower, P. A. D. Goncalves, N. A. Mortensen, and J. B. Khurgin, "Plasmonic silicon Schottky photodetectors: The physics behind graphene enhanced internal photoemission," *APL Photon.*, vol. 2, no. 2, Feb. 2017, Art. no. 026103.

[45] S. P. Sundararaian, N. K. Grady, N. Mirin, and N. J. Halas, "Nanoparticle-induced enhancement and suppression of photocurrent in a silicon photodiode," *Nano Lett.*, vol. 8, no. 2, pp. 624–630, Feb. 2008.

[46] P. Matheu, S. H. Lim, D. Derkacs, C. McPheeters, and E. T. Yu, "Metal and dielectric nanoparticle scattering for improved optical absorption in photovoltaic devices," *Appl. Phys. Lett.*, vol. 93, no. 11, Sep. 2008.

[47] L. Liu *et al.*, "Silicon waveguide grating coupler for perfectly vertical fiber based on a tilted membrane structure," *Opt. Lett.*, vol. 41, no. 4, pp. 820–823, Feb. 2016.

[48] D. Vercruysse, P. Neutens, L. Lagae, N. Verellen, and P. Van Dorpe, "Single asymmetric plasmonic antenna as a directional coupler to a dielectric waveguide," *ACS Photon.*, vol. 4, no. 6, pp. 1398–1402, Jun. 2017.

[49] M. S. Nisar, X. Zhao, A. Pan, S. Yuan, and J. Xia, "Grating coupler for an on-chip lithium niobate ridge waveguide," *IEEE Photon. J.*, vol. 9, no. 1, Feb. 2017, Art. no. 6600208.

[50] X. M. Wang, Z. Z. Cheng, K. Xu, H. K. Tsang, and J. B. Xu, "High-responsivity graphene/silicon-heterostructure waveguide photodetectors," *Nature Photon.*, vol. 7, no. 11, pp. 888–891, Nov. 2013.

[51] J. Q. Wang *et al.*, "High-responsivity graphene-on-silicon slot waveguide photodetectors," *Nanoscale*, vol. 8, no. 27, pp. 13206–13211, 2016.

[52] A. V. Krishnamoorthy and D. A. B. Miller, "Scaling optoelectronic-VLSI circuits into the 21st century: A technology roadmap," *IEEE J. Select. Topics Quantum Electron.*, vol. 2, no. 1, pp. 55–76, Apr. 1996.

[53] P. Wahl *et al.*, "Energy-per-bit limits in plasmonic integrated photodetectors," *IEEE J. Sel. Topics Quantum Electron.*, vol. 19, no. 2, pp. 3800210–3800210, Mar./Apr. 2013.

[54] S. M. Sze and K. K. Ng, *Physics of Semiconductor Devices*. New York, NY, USA: Wiley, 2007.

[55] W. F. Brinkman, R. C. Dynes, and J. M. Rowell, "Tunneling conductance of asymmetrical barriers," *J. Appl. Phys.*, vol. 41, no. 5, 1970, Art. no. 1915.

[56] S. Cova, M. Ghioni, A. Lacaita, C. Samori, and F. Zappa, "Avalanche photodiodes and quenching circuits for single-photon detection," *Appl. Opt.*, vol. 35, no. 12, pp. 1956–1976, Apr. 1996.

[57] G. Konstantatos *et al.*, "Hybrid graphene-quantum dot phototransistors with ultrahigh gain," *Nature Nanotechnol.*, vol. 7, no. 6, pp. 363–368, Jun. 2012.

[58] Y. J. Ma *et al.*, "Tailoring the performances of low operating voltage InAlAs/InGaAs avalanche photodetectors," *Opt. Express*, vol. 23, no. 15, pp. 19278–19287, Jul. 2015.

[59] H. Tan *et al.*, "Single-crystalline InGaAs nanowires for room-temperature high-performance near-infrared photodetectors," *Nano-Micro. Lett.*, vol. 8, no. 1, pp. 29–35, Jan. 2016.

[60] B. Desiatov *et al.*, "Plasmonic enhanced silicon pyramids for internal photoemission Schottky detectors in the near-infrared regime," *Optica*, vol. 2, no. 4, pp. 335–338, 2015.

[61] T. Mueller, F. N. A. Xia, and P. Avouris, "Graphene photodetectors for high-speed optical communications," *Nature Photon.*, vol. 4, no. 5, pp. 297–301, May 2010.

[62] O. Lopez-Sanchez *et al.*, "Light generation and harvesting in a van der waals heterostructure," *ACS Nano*, vol. 8, no. 3, pp. 3042–3048, Mar. 2014.

[63] A. Sobhani *et al.*, "Enhancing the photocurrent and photoluminescence of single crystal monolayer MoS2 with resonant plasmonic nanoshells," *Appl. Phys. Lett.*, vol. 104, no. 3, Jan. 2014, Art. no. 031112.

[64] K. F. Mak, C. Lee, J. Hone, J. Shan, and T. F. Heinz, "Atomically thin MoS2: A new direct-gap semiconductor," *Phys. Rev. Lett.*, vol. 105, no. 13, Sep. 2010.

[65] M. Chhowalla *et al.*, "The chemistry of two-dimensional layered transition metal dichalcogenide nanosheets," *Nature Chem.*, vol. 5, no. 4, pp. 263–275, Apr. 2013.

[66] J. Ryou, Y. S. Kim, K. C. Santosh, and K. Cho, "Monolayer MoS_2 bandgap modulation by dielectric environments and tunable bandgap transistors," *Sci. Rep.*, vol. 6, Jul. 2016, Art. no. 29184.

[67] C. P. Byers *et al.*, "From tunable core-shell nanoparticles to plasmonic drawbridges: Active control of nanoparticle optical properties," *Sci. Adv.*, vol. 1, no. 11, Dec. 2015, Art. no. e1500988.

[68] F. P. G. de Arquer, F. J. Beck, M. Bernechea, and G. Konstantatos, "Plasmonic light trapping leads to responsivity increase in colloidal quantum dot photodetectors," *Appl. Phys. Lett.*, vol. 100, no. 4, Jan. 2012, Art. no. 043101.

[69] J. A. Tang and E. H. Sargent, "Infrared colloidal quantum dots for photovoltaics: Fundamentals and recent progress," *Adv. Mater.*, vol. 23, no. 1, pp. 12–29, Jan. 2011.

[70] J. Ma and L. W. Wang, "The nature of electron mobility in hybrid perovskite CH3NH3PbI3," *Nano Lett.*, vol. 17, no. 6, pp. 3646–3654, Jun. 2017.

[71] Z. H. Sun, L. Aigouy, and Z. Y. Chen, "Plasmonic-enhanced perovskite-graphene hybrid photodetectors," *Nanoscale*, vol. 8, no. 14, pp. 7377–7383, 2016.

[72] X. Wan *et al.*, "A self-powered high-performance graphene/silicon ultraviolet photodetector with ultra-shallow junction: breaking the limit of silicon?," *Npj 2d Mater. Appl.*, vol. 1, Apr. 2017.

[73] Y. Salamin *et al.*, "High speed photoconductive plasmonic germanium detector," in *Proc. Conf. Lasers Electro-Optics*, 2017, Paper STu1N.2.

[74] Y. Salamin *et al.*, "100 GHz plasmonic photodetector," *ACS Photon.*, to be published.

[75] I. Goykhman *et al.*, "On-chip integrated, silicon-graphene plasmonic schottky photodetector with high responsivity and avalanche photogain," *Nano Lett.*, vol. 16, no. 5, pp. 3005–3013, May 2016.

[76] D. Schall *et al.*, "Record high bandwidth integrated graphene photodetectors for communication beyond 180 Gb/s," in *Proc. Opt. Fiber Commun. Conf.*, 2018, Paper M2I.4.

[77] P. Ma *et al.*, "Plasmonically enhanced 100 Gbit/s graphene photodetector," submitted for publication.

[78] B. Y. Zheng, Y. M. Wang, P. Nordlander, and N. J. Halas, "Color-selective and CMOS-compatible photodetection based on aluminum plasmonics," *Adv. Mater.*, vol. 26, no. 36, pp. 6318–6323, Sep. 2014.

[79] M. W. Knight *et al.*, "Aluminum for plasmonics," *ACS Nano*, vol. 8, no. 1, pp. 834–840, Jan. 2014.

[80] S. C. Lee, S. Krishna, and S. R. J. Brueck, "Light direction-dependent plasmonic enhancement in quantum dot infrared photodetectors," *Appl. Phys. Lett.*, vol. 97, no. 2, Jul. 2010.

[81] S. J. Lee *et al.*, "A monolithically integrated plasmonic infrared quantum dot camera," *Nat. Commun.*, vol. 2, Apr. 2011, Art. no. 286.

[82] P. Fan *et al.*, "An electrically-driven GaAs nanowire surface plasmon source," *Nano Lett.*, vol. 12, no. 9, pp. 4943–4947, 2012.

[83] O. Lotan *et al.*, "Propagation of channel plasmons at the visible regime in aluminum V-groove waveguides," *ACS Photon.*, vol. 3, no. 11, pp. 2150–2157, 2016.

[84] E. Bermúdez-Ureña *et al.*, "Plasmonic waveguide-integrated nanowire laser," *Nano Lett.*, vol. 17, no. 2, pp. 747–754, 2017.

[85] J.-H. Kang *et al.*, "Defect-free GaAs/AlGaAs core–shell nanowires on Si substrates," *Crystal Growth Design*, vol. 11, no. 7, pp. 3109–3114, 2011.
[86] A. M. Munshi *et al.*, "Position-controlled uniform GaAs nanowires on silicon using nanoimprint lithography," *Nano Lett.*, vol. 14, no. 2, pp. 960–966, Feb. 2014.
[87] T. Rieger et al., "Simultaneous integration of different nanowires on single textured Si (100) substrates," *Nano Lett.*, vol. 15, pp. 1979–1986, 2015.
[88] E. Russo-Averchi *et al.*, "High yield of GaAs nanowire arrays on Si mediated by the pinning and contact angle of Ga," *Nano Lett.*, vol. 15, no. 5, pp. 2869–2874, May 2015.
[89] K. Tomioka, Y. Kobayashi, J. Motohisa, S. Hara, and T. Fukui, "Selective-area growth of vertically aligned GaAs and GaAs/AlGaAs core-shell nanowires on Si(111) substrate," *Nanotechnology*, vol. 20, no. 14, Apr. 2009.
[90] J. Noborisaka, J. Motohisa, and T. Fukui, "Catalyst-free growth of GaAs nanowires by selective-area metalorganic vapor-phase epitaxy," *Appl. Phys. Lett.*, vol. 86, no. 21, May 2005.

Alexander Dorodnyy received B.S. and M.S. from the Moscow Institute of Physics and Technology, Dolgoprudny, Russia, in 2009 and 2011, respectively, and the Ph.D. degree from the Department of Information Technology and Electrical Engineering, ETH Zurich, Zurich, Switzerland, in 2016.

Since 2016, he has been a Postdoctoral Researcher with the Institute of Electromagnetic Fields, ETH Zurich. His research interests include photovoltaic devices, photodetectors, plasmonic devices, tele-/data-communication components, photonic metasurfaces, applications of nanowire structures, numerical methods for photonics, carrier dynamics in solid-state materials, and numerical optimization techniques.

Yannick Salamin (S'13) received the B.S. degree in electrical engineering from the University of Applied Science of Western Switzerland, Sion, Switzerland, in 2010, and the M.S. degree in electrical engineering from Zhejiang University, Hangzhou, China, in 2014. He is currently working toward the Ph.D. degree at ETH Zurich, Zurich, Switzerland.

As a Visiting B.S. Student, he visited Zhejiang University for six months in 2010. From 2011 to 2014, he was with the Laboratory of Applied Research on Electromagnetic, Zhejiang University. Since 2014, he has been with the Institute of Electromagnetic Fields, ETH Zurich, Zurich, Switzerland. His research interests include electro-optic devices, plasmonics, microwave photonics, and metamaterials.

Mr. Salamin was the recipient of a full scholarship for postgraduate studies granted by the Ministry of Education of China (2011–2014).

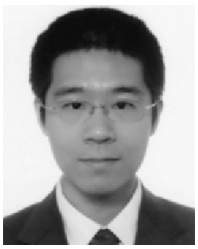

Ping Ma received the B.E. degree from Tianjin University, Tianjin, China, in 2003, the M.Sc. degree from the Royal Institute of Technology, Stockholm, Sweden, in 2005, and the D.Sc. degree from the Swiss Federal Institute of Technology Zurich (ETH), Zürich, Switzerland, 2011. His doctoral thesis studied photonic bandgap structures with TM-bandgap for ultrafast all-optical switches based on intersubband transition in InGaAs/AlAsSb quantum wells. After a short postdoctoral research stay at ETH Zurich, he was with Oracle Labs in San Diego, CA, USA, where he performed research on ferroelectric materials for spectral tuning of ring resonators and novel electro-optic modulators for silicon photonic interconnects. He has recently returned to ETH Zurich and joined in Prof. Juerg Leuthold's Institute, as a Senior Research Scientist. He is the author or coauthor of 14 publications and holds one pending patent.

Jelena Vukajlovic Plestina was born in Mali Losinj, Croatia, 1982. She studied physics at the Faculty of Science, University of Zagreb, received the Master's degree in 2010, and the Ph.D. degree in the position-controlled nanowire growth on silicon substrates, in 2017, from the Laboratory of Semiconductor Materials, École Polytechnique Fédérale de Lausanne, Lausanne, Switzerland, where she is currently a Postdoctoral Researcher. After graduation, she was a physics high school Teacher and also worked in STEM-oriented education development.

Nolan Lassaline was born near Toronto, ON, Canada, in 1991. He received the Bachelor of Science degree in nanotechnology engineering from the University of Waterloo, Waterloo, ON, Canada, in 2014, and the Master of Science degree in micro- and Nanosystems from ETH Zürich, Zürich, Switzerland, in combination with the IBM Zürich Research Laboratory. He is currently working toward the Doctoral degree in the Optical Materials Engineering Laboratory, ETH Zürich, under the supervision of Professor David Norris.

His research interests include nanoscale optical materials, which lie at the intersection of chemistry, physics, and engineering, the study of fundamental physical phenomena and material properties, and fabrication and engineering of nanophotonic structures and devices.

Dmitry Mikulik received the Bachelor's and Master's degrees in physics from St. Petersburg Electro-Technical University, Saint Petersburg, Russia, in 2005 and 2007, respectively. He is currently working toward the Ph.D. degree in the development III-V NW-based solar cells in École Polytechnique Fédérale de Lausanne (EPFL), Lausanne, Switzerland. He was a Junior Researcher with Ioffe Institute, Saint Petersburg, Russia, until 2012. Prior to moving to EPFL, he spent three years as a Senior Engineer with Samsung Electronics, Suwon, South Korea, working on different semiconductor epitaxial processes.

Pablo Romero-Gomez was born in Cordoba, Spain, in 1983. He received the B.S. degree in physics from the University of Cordoba, Córdoba, Spain, in 2006, and the Ph.D. degree from the University of Seville, Seville, Spain, in 2011.

From 2011 to 2016, he was a Postoctoral Researcher with the Organic Nanostructured Photovoltaics Laboratory. Since 2016, he has been a Scientist with the Laboratory of Semiconductor Materials, École Polytechnique Fédérale de Lausanne, Lausanne, Switzerland. He has participated in 12 Projects (four of them European-Union-funded projects), and was the author or coauthor of 32 articles in peer-reviewed international journals of high impact factor (more than 80% in Q1, 11 as first author, and more than 25 coauthor worldwide). Detailed information of his publications can be found in Scholar List of Publications (https://goo.gl/uiDA4X). To date he has an h-index of 16, with more than 700 citations. His works have been presented at 34 international recognized conferences mostly in Europe and USA. He is also the coauthor of one of the most prestigious books completely focused on Industrial Plasma Technology: "Applications from Environmental to Energy Technologies" published by Wiley. His experience in technology transfer is corroborated by the fact that he has four patents (one licensed by Cosentino). In addition, his results developed during his postdoctoral research were elected as the finalist of the "Vanguardia de la Ciencia 2014" award.

Anna Fontcuberta i Morral was born in Barcelona in 1975. She received the Diploma in physics from the University of Barcelona, Barcelona, Spain, in 1997, and the Ph.D. degree in materials Science from Ecole Polytechnique, Palaiseau, France, 2001.

She then moved with the Group of Harry Atwater at CalTech, where she co-started the company Aonex Technologies. From 2005 to 2010, she was a Group Leader with the Walter Schottky Institut, TU Munich. In 2008, she was with the École Polytechnique Fédérale de Lausanne, where she is currently an Associate Professor and Head of the Laboratory of Semiconductor Materials. Her research interests include the synthesis and characterization of novel materials, including in the form of nanostructures, and their application in quantum computing, photodetectors, and solar cells. She is especially interested in the sustainable use of materials, including the search of earth abundant direct-bandgap semiconductors.

Juerg Leuthold (F'13) was born in 1966 in Switzerland. He received the Ph.D. degree in physics from ETH Zürich, Zürich, Switzerland, for work in the field of integrated optics and all-optical communications. From 1999 to 2004, he was with Bell Labs, Lucent Technologies, Holmdel, NJ, USA, where he has been performing device and system research with III/V semiconductor and silicon optical bench materials for applications in high-speed telecommunications. From 2004 to 2013, he was a Full Professor with Karlsruhe Institute of Technology, where he headed the Institute of Photonics and Quantum Electronics and the Helmholtz Institute of Microtechnology. Since March 2013, he has been a Full Professor with Swiss Federal Institute of Technology (ETH Zürich), Zürich, Switzerland.

He is a fellow of the Optical Society of America. While being a Professor at the KIT, he was a member of the Helmholtz Association Think Tank and a member of the Heidelberg Academy of Science. He currently serves as a Board of Director in the Optical Society of America. He has been and is serving the community as the general chair in many technical program committees.